EELS study of the inverse martensitic transformation of 2H and 18R Cu–Al–Zn alloys

F. Espinosa-Magaña, M.T. Ochoa-Lara, F. Lovey, H. Flores-Zúñiga, D. Ríos-Jara

Abstract

Changes in 3d states occupancy associated with the inverse martensitic transformation in two samples of Cu–Al–Zn alloys with 2H and 18R martensitic structures were investigated by electron energy loss spectroscopy (EELS). The Cu L2,3 white-lines intensities, which reflect the unoccupied density of states in 3d bands, were measured in situ, during the phase transformation in both the martensite and austenite phases. We find that the white-lines intensity decreases during the inverse transformation, when going from martensite to austenite. Even though the initial 3d occupation numbers in 2H and 18R martensitic structures are different, after the transformation, the 3d occupation numbers in the now austenitic structure have decreased in both samples, indicating that some electrons left Cu 3d bands during phase transformation. Interestingly enough, the occupation numbers in the final phases, which have the same structure, reach the same value, indicating that changes in EELS spectra are a consequence of structural changes.

Keywords: EELS, Electronic structure, Cu-Al-Zn, White lines.

Introduction

As is well known, β Hume–Rothery alloys and specially those based on Cu, exhibit shape memory and superelasticity phenom- ena, closely associated to the thermoelastic martensitic transfor- mation [1], as well as with alloy composition. These

alloys present a sequence of phases on cooling being the stability of each one governed by electron concentration *e/a* [2], the average number of conduction electrons per atom. Therefore, martensitic transfor- mation is associated with this succession of phases in cooling from A2 structure to martensitic phase. Austenitic β phase shows several types of chemical ordering [3]: A2 phase which is present at elevated temperature and shows a disordered BCC structure; on cooling below the eutectoid temperature, this phase undergoes a transition to B2 order, exhibiting a CsCl structure, and at even lower temperatures, appears a DO3 (stoichiometry $CuAl_3$). Finally, after the cooling process, the martensitic phase starts its formation below the characteristic Ms temperature. On heating, martensitic to austenitic or inverse martensitic transformation occurs.

Martensitic transformation, which is a very important process for inducing shape memory effect, can take place on different martensitic structures, which depends strongly on the alloy composition. Some typical martensitic phases that can be obtained are 9R, 18R and 2H structures, where the number and the letter indicate the stacking period and the structure symmetry, respectively, R: rhombohedral and H: hexagonal [4–6]. In this work, the inverse martensitic transformation and the electronic structure changes on 2H or γ_1' (hexagonal) and 18R or b1' (rhombohedral) structures are studied.

Even though it has been long recognized that the electronic structure plays an important role in the study of phase transformations, these kinds of studies are not a common issue in the literature. In this article we studied the changes in electronic structure associated with an in situ generated inverse martensitic transformation in two

Cu–Al–Zn alloys. To our knowledge, EELS has not been used for studies of Cu–Al–Zn alloys yet.

Theory

Electron energy loss spectroscopy (EELS) is a powerful analytical technique that can be utilized to obtain information on the structure, bonding and electronic properties of a material [7–13]. The interactions of fast electrons with the specimen result in excitations of electrons into unoccupied energy levels in the conduction band as well as collective excitations of valence electrons. When a spectrum is obtained by analyzing the energy lost by the incident electrons, the region up to an energy loss of ~50 eV is dominated by collective excitations of valence electrons (plasmon) and by interband transitions. At higher energy losses ionization edges occur due to excitation of core electrons into the conduction band.

The excitation of atomic inner shells by high energy electrons provides a method for studying the unoccupied conduction states in a solid. These core-level processes are mostly sensitive to final states since the initial states have narrow energy widths. Besides the well defined ionization edges there is a fine structure superposed on the edge and extending up to about 50 eV from the edge onset, which is associated with the density of unoccupied states in the conduction band, known as the energy loss near edge structure (ELNES).

In case of 3d transition metals as well as their alloys, $L_{2,3}$ edges of EELS are characterized by two sharp peaks, known as "white lines". Because the predominance of dipole transitions, these white lines originate mainly from excitations of $2p_{1/2}$ and $2p_{3/2}$ core electrons to unoccupied d-like states near the Fermi level. The white-lines

intensities reflect the unoccupied 3d density of states (DOS). Data on the occupancies of 3d and 4d states can clarify many issues fundamental to electronic theories of transition metal alloys, including phase transformations.

The 3d and 4d occupations of transition metals have been studied systematically by several authors [14–22]. Pearson et al. [14] have attempted to relate the sum of the L_3 and L_2 white-lines intensities to the occupancies of the corresponding outer d states, and Hernandez et al. [23] studied changes in occupation number in Cu 3d orbitals during the martensitic transformation in Cu– Al–Be alloy. The experimental studies on the white lines from $L_{2,3}$ EELS spectra for elemental metals of the 3d transition series found that the normalized intensities of these white lines decreased nearly linearly with increasing d-state occupancy across the series. The normalized white-line intensity was defined as the integrated intensity of the L_2 and L_3 white lines divided by the integrated intensity in a normalization window 50 eV in width beginning 50 eV past the L_3 edge onset. When the normalized white-line intensities for the 3d metals were divided by appro- priate matrix-element correction factors, which were calculated for each atomic species, a linear correlation with 3d occupancy was obtained with a fit given by

$$I'_{3d} = 10.8(1 - 0.1n_{3d}) \tag{1}$$

where I^0_{3d} is the normalized white-line intensity divided by the appropriate matrix-element correction factor and n_{3d} is the 3d occupancy in electron/atom. The above correlation between the normalized white-line intensity and 3d occupancy (electron/ atom) is useful for determining changes in outer d state occupancy upon

alloying and solid-state phase transformations if the corresponding changes in the normalized white-line intensity are observed.

Experimental

TEM and EELS studies were performed on Cu-23.22 at% Al-6.44 at% Zn (martensite 2H, Ms = 50 °C) and Cu-17.97 at% Al-12.6 at% Zn (martensite 18R, Ms = 50 °C) alloys, which will be labeled as alloy1 and alloy2, respectively.

Alloys were prepared from high purity aluminum, copper and zinc elements, by melting in a high frequency furnace under an argon atmosphere. Then, single crystals were grown by a modified Bridgman method. Thin and disc shape specimens with 3 mm diameter, were cut from alloys and prepared for TEM analysis with a double jet electrochemical thinner.

Electron energy loss spectroscopy (EELS) was used to study the transitions from martensitic to austenitic phases in both alloys by placing the samples in a TEM heating sample holder and measuring the changes in electronic structure of element copper during an *in-situ* heating process from room temperature to 120 °C. EELS spectra were obtained using a Gatan Parallel Electron Energy Loss Spectrometer (PEELS model 766) attached to a Philips CM200 transmission electron microscope (TEM). Spectra were taken in diffraction mode with 0.2 eV/ch dispersion, an aperture of 3 mm and a collection semi-angle of 2.8 mrad. The resolution of the spectra was determined by measuring the full width at half- maximum (FWHM) of the zero-loss peak and this was typically close to 1.5 eV, when the TEM was operated at 200 kV. The EELS spectra were corrected for dark current and readout noise. The channel to channel gain variation was minimized by normalizing the experimental spectrum with independently

obtained gain spectrum of the spectrometer. All spectra were examined for oxygen edges to prevent any surface oxides.

Spectra were background-subtracted by fitting the pre-edge backgrounds with a power-law function and then Fourier-ratio deconvoluted to remove multiple scattering components from the spectra. Several spectra were obtained from four different samples for every structure and at least two regions in every sample.

Results and discussion

To characterize the phases involved in the transformations, TEM observations were performed at room temperature and 120 °C, when we were convinced that the inverse martensitic transformation had taken place, by observing bright field images and diffraction patterns in both samples, before and after the heating processes. Fig. 1 shows the evolution from 2H structure (Fig. 1a), at room temperature to β phase structure (Fig. 1c), at 120 °C and from 18R structure (Fig. 1b), at room temperature to b structure (Fig. 1d), at 120 °C. Figs. 1a and c show micrographs and diffraction patterns which are characteristic of martensitic structures, whereas Figs. 1c and d show diffraction patterns from [0 11] and [111] zone axes, which are characteristic of β phase structure.

EELS spectra were obtained from alloy1 and alloy2 before and after the heating process, taking care to acquire spectra on the same area in every sample, in order to prevent the acquisition of spectra from different orientations and thicknesses that could obscure our analysis.

To extract the white lines from copper atoms, we closely follow the empirical method developed by Pearson et al. [16]. The $L_{2,3}$-edge is composed of two

independent overlapping L_2 and L_3-edges, resulting from transitions from 2p states into bound 3d, and continuum states. In Pearson's model, the aim is to isolate the transitions to bound states and to eliminate transitions to the continuum. In order to subtract transitions to the continuum, the background is modeled with a double step function. A straight line is fit to the background immediately following the L_2 white line by choosing the first flat region with at least 10 eV width. This line is extrapolated into the threshold region and then modified into a double step of the same slope with onsets occurring at the white-line maxima. The ratio of the step heights is chosen as 2:1 which is the multiplicity of the initial steps (four $2p_{3/2}$ electrons and two $2p_{1/2}$ electrons).
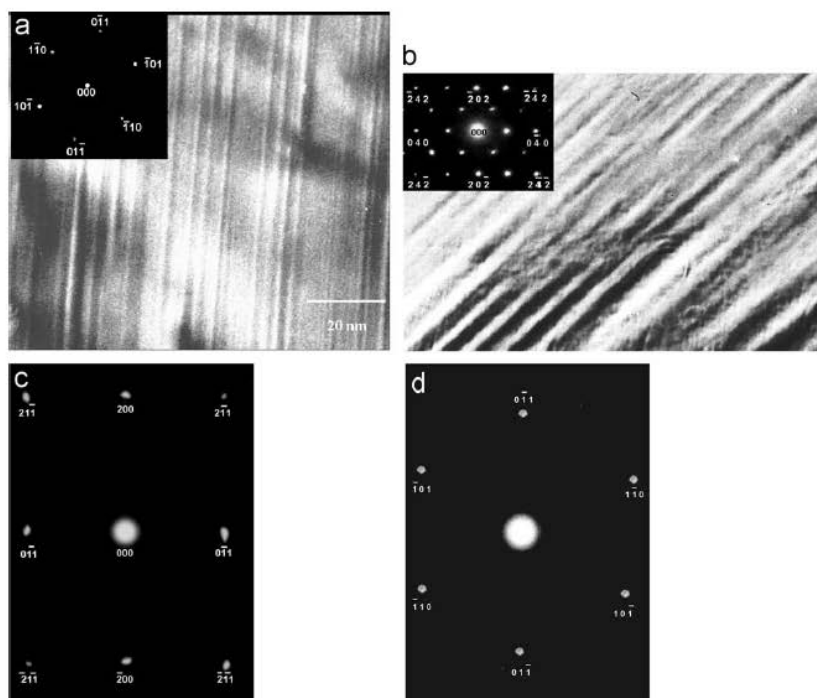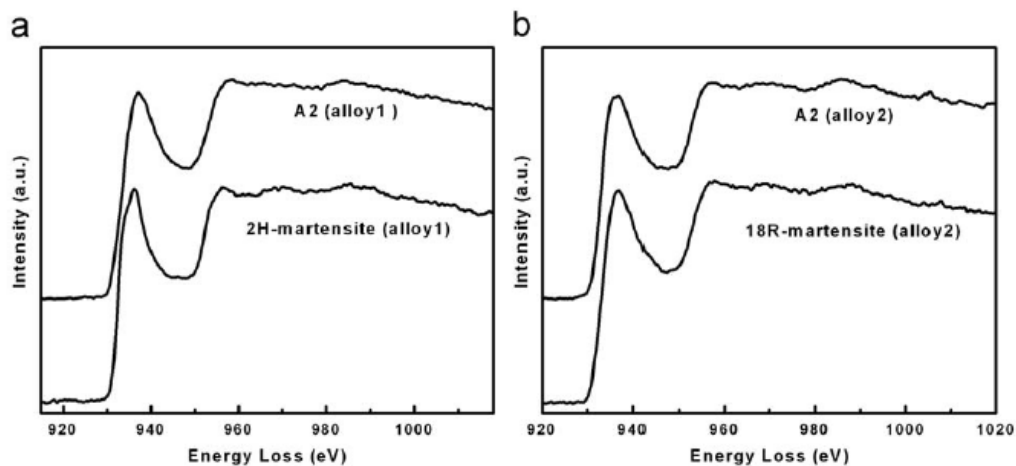

Fig. 1. (a) TEM image and diffraction pattern taken from zone axis $[\bar{1}\,\bar{1}\,\bar{1}]_{2H}$ of alloy1. (b) TEM image and diffraction pattern from zone axis $[1\,0\,1]_{18R}$ of alloy2. (c) Diffraction pattern from zone axis $[0\,1\,1]_\beta$ after heating, obtained from alloy1. (d) Diffraction pattern from zone axis $[1\,1\,1]_\beta$ after heating, obtained from alloy2.

Fig. 2. (a) Superposition of Cu $L_{2,3}$ edges from 2H-martensite (black) and A2-austenite (red) structures in alloy1. (b) Superposition of Cu $L_{2,3}$ edges from 18R-martensite (black) and A2-austenite (red) structures in alloy2. (For interpretation of the refrences to color in this figure legend, the reader is referred to the web version of this article.)

The white-lines area is then divided by the area in a normalization window 50 eV in width, beginning 50 eV past the onset of the L_3 white line, which yields normalized white-line intensity for the alloy. Following the above steps is important if we want to use the linear relationship between normalized L_2 and L_3 areas and 3d occupation number, derived by Pearson et al. [14–16]. Dividing by the matrix-element factor, that is 0.172 for copper, and using Eq. (1) allows us to obtain Δn_{3d} in electron/atom for the transitions.

Figs. 2 a and b show energy-loss spectra for Cu $L_{2,3}$ ionization edges during the transition from martensite to b structure in both, 2H martensite (alloy1) and 18R martensite (alloy2) starting from martensite structures, respectively, where spectra were shifted up for clarity. After background-subtracted and Fourier-ratio deconvoluted, spectra were aligned so that the value of the threshold energy, measured at one tenth of the half-height of the L_3 white line, was at 931 eV. We did not attempt to measure chemical shifts of the absorption edges due to these transitions as they are very small (within the experimental resolution).

Fig. 3 illustrates the procedure outlined above, from one of the samples, to extract white-lines intensities, showing the double step fit to $L_{2,3}$ white lines. The area under the spectrum and above the double step is associated to the white-lines intensity.

Results of the normalized white-lines intensities and occupa- tion number in 3d orbitals for Cu atoms, are summarized in Table 1 for the two samples. It is observed a small, but otherwise measurable, charge transfer when going from martensite to β structure.
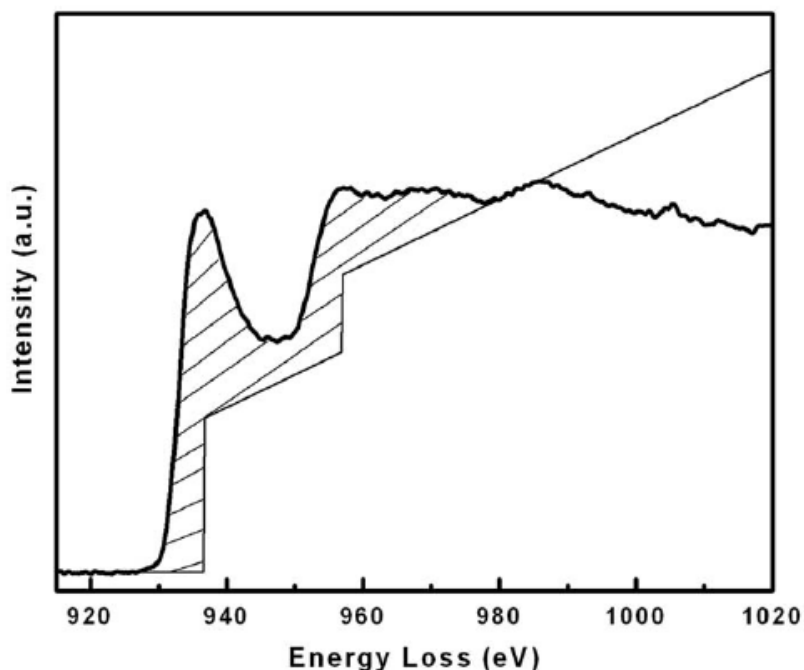

Fig. 3. An EELS spectrum acquired from A2-austenite in alloy2, showing the technique used to extract the intensity of white lines (hatched area).

Table 1
Results obtained for the white lines normalized intensities and 3d electron occupancy during the inverse martensitic transformation in 2H and 18R structures.

Structure	$L_{2,3}$	n_{3d}
alloy1 (2H)	0.146	9.21
alloy1 (A2)	0.197	8.94
alloy2 (18R)	0.175	9.06
alloy2 (A2)	0.199	8.93

For alloy1, in the transition from 2H martensite to austenite b, copper loses 0.27 electron/atom, while in the alloy2, when going from 18R martensite to β, copper loses 0.13 electron/ atom. As these values are greater than our maximum statistical uncertainty of 0.08 electron/atom, as estimated from our analyzed spectra acquired from four different samples and at least two regions in every sample, as mentioned above (Pearson's associated uncertainty is 0.06 electron/atom), we can conclude that a charge transfer takes place during these diffusionless transitions. However, the most important remark on these results is the fact that, starting from two different martensitic structures with two different occupation numbers, namely 9.21 and 9.06 electron/atom in 3d orbitals for alloy1 (2H) and alloy2 (18R), respectively, we ended with two austenite structures (β phase) with the same occupation number, within our uncertainty, in 3d orbitals: 8.94 and 8.93 electron/atom in alloy1 and in alloy2, respectively.

It is generally believed that changes in the local electronic structure are the result of local compositional and structural differences, being the chemical effect superior over the structural one. In martensitic transformation, which is a diffusionless process, no appreciable changes would be expected in the electronic structure due to chemical changes. However, our results imply that the structural changes associated with the martensitic transformation are responsible for the measured difference in the Cu white-lines intensities between the two phases, despite other hybridization effects.

Conclusions

Changes in the electronic structure during the inverse martensitic transformation in two samples of Cu–Al–Zn alloys were studied by electron energy loss spectroscopy, by analyzing the changes in Cu $L_{2,3}$ white-lines intensity in 2H and 18R martensitic

structures. It was found that about 0.27 electron/atom left Cu 3d states, after the inverse martensitic transformation in 2H structure, when going from martensite to austenite and about. 0.13 electron/atom left Cu 3d states after the inverse martensitic transformation in 18R structure. Even though changes in $L_{2,3}$ intensities from copper atoms are small, these results can help to elucidate the controversy on the electronic changes during structural changes.

References

[1]   Z. Nishiyama, Martensitic transformations, Academic Press, London, 1978.

[2]   C.S. Barret, T.B. Massalski, Structure of Metals, third ed., McGraw-Hill, New York, 1996.

[3]   M. Jurado, T. Castan, L. Man˜osa, A. Planes, J. Bassas, Alcobe' , M. Morin, Philos. Mag. A 75 (1997) 1237.

[4]   K. Otsuka, T. Ohba, M. Tokonami, C.M. Wayman, Scr. Metall. Mater. 29 (1993) 1359.

[5]   L. Delaey, M. Chandrasekara, Scr. Metall. Mater. 30 (1994) 1605.

[6]   T. Saburi, C.M. Wayman, Acta. Metall. 27 (1979) 979.

[7]   R.F. Egerton, in: Electron Energy Loss Spectroscopy in the Electron Microscope, second ed., Plenum Press, New York, 1996.

[8]   M.M. Disko, C.C. Ahn, B. Fultz, in: C.C. Ahn (Ed.), Transmission Electron Energy Loss Spectrometry Materials Science, second ed., WILEY-VCH Verlag GmbH & Co. KGaA, Warrendale, Pennsylvania, 2004.

[9]   G. Soto, E.C. Samano, R. Machorro, M.H. Farı́as, L. Cota-Araiza, Appl. Surf. Sci. 183 (2001) 246.

[10]   K. van Benthem, C. Elsä sser, J. Appl. Phys. 90 (2001) 6156.

[11]   K. van Benthem, R.H. French, W. Sigle, C. Elsä sser, M. Rü hle, Ultramicroscopy 86 (2001) 303.

[12]   G. Brockt, H. Lakner, Micron 31 (2000) 435.

[13] S.M. Bose, Phys. Rev. Lett. A 289 (2001) 255.

[14]   D.H. Pearson, B. Fultz, C.C. Ahn, Appl. Phys. Lett. 53 (1988) 1405.

[15]   D.H. Pearson, C.C. Ahn, B. Fultz, Phys. Rev. B 47 (1993) 8471.

[16]   D.H. Pearson, C.C. Ahn, B. Fultz, Phys. Rev. B 50 (1994) 12969.

[17]   G.Y. Yang, J. Zhu, J. Magn. Magn. Mater. 220 (2000) 65.

[18]   P.L. Potapov, S.E. Kulkova, D. Schryvers, J. Verbeeck, Phys. Rev. 64 (2001) 184110.

[19]   G.A. Botton, G.Y. Guo, W.M. Temnerman, C.J. Humphreys, Phys. Rev. B 54 (1996) 1682.

[20]   Y. Murakami, D. Shindo, K. Otsuka, T. Oikawa, J. Electron Microsc. 47 (1998) 301.

[21]   R.D. Leapman, L.A. Grunes, P.L. Fejes, Phys. Rev. B 26 (1982) 614.

[22]   T.G. Sparrow, B.G. Williams, C.N.R. Rao, J.M. Thomas, Chem. Phys. Lett. 108 (1984) 547.

[23]   J.H. Herna' ndez, M.T. Ochoa-Lara, H. Flores-Zuñiga, F. Espinosa-Magaña, D.

Rı́os-Jara, J. Electro´ n Spectrosc. Relat. Phenom. 151 (2006) 149.